C_{60} Molecular Bearings and the Phenomenon of Nanomapping

T. Coffey* and J. Krim

Physics Department, North Carolina State University, Box 8202, Raleigh, North Carolina 27695, USA

(Received 2 January 2006; published 11 May 2006)

Inspired by suggestions of C_{60} ''nanobearings,'' we have measured sliding friction on fixed and rotating C_{60} layers to explore whether a lubricating effect is present. We refer to this general phenomenon as ''nanomapping,'' whereby macroscopic attributes are mapped in a one on one fashion to nanoscale entities. Our measurements are the first to directly link friction to a documented molecular rotation state. Friction is, however, observed to be *higher* for rotating layers, in defiance of the ball-bearing analogy. Thus, no direct mapping of macro- to nanoscale attributes can be established.

DOI: 10.1103/PhysRevLett.96.186104 PACS numbers: 68.35.Af, 68.43.Pq, 68.60.−p

''Nanomapping'' abounds in the present day literature, particularly so in discussions of nanoscale machine design [1–4]. We define it here as a direct one on one linkage of macroscopic and nanoscale attributes, irrespective of whether there exists a scientific basis for the linkage. ''Top-down'' mapping casts atomic-scale machines as miniature versions of their macroscopic analogs, the expectation being that they might perform similarly [1]. ''Bottom-up'' mapping links the performance of an atomic-scale system to a macroscopic system of which it is reminiscent [2,3,5]. Of course, there should be nanomapping if the ingredients of the macroscale and nanoscale systems are the same. However, one needs to carefully check the ingredients before making the claim that there should be nanomapping [6]. We examine here the common notion of C_{60} as a ''nanobearing,'' to shed light on current debate over whether nanomapping is a rational design approach or simply coincidental.

C_{60} is a ''soccer ball'' shaped molecule whose spherical shape, chemical stability, and rotational motion within solid-phase lattices suggest that it might prove highly effective as a lubricant. While C_{60} has proven to be disappointing overall as a lubricant, Miura *et al.* recently reported that C_{60} molecular layers confined between graphite layers did act as molecular ball bearings [5]. In that work, a stick-slip model for C_{60} molecules was proposed to explain the observed low friction levels. The experiment inspired much theoretical study [4,7], but rotation of the C_{60} molecules was not definitively established. For example, molecular dynamics simulations by Legoas *et al.* [7] showed that the stacking of the molecular layers (termed AB stacking in the paper) was assumed to be present but was not observed and that the main experimental features could be explained without invoking a stick-slip process. Lateral force microscopy (LFM) studies of C_{60} surfaces in rapid and repressed rotational states, moreover, have revealed increased adhesion for the repressed rotational states but no difference in friction [8,9]. Links between known rotational states and experimentally measured sliding friction levels for C_{60}, as well as other spherical molecules [10,11], have thus remained unproven. We have employed a quartz crystal microbalance, which probes shorter time scales than LFM, to measure friction levels for molecularly thin methanol films sliding along C_{60} substrates in rapid and repressed rotational states. We report herein our experimental observation of *increased* friction for the case of rapid rotation, in defiance of the ball-bearing analogy.

C_{60} is a remarkably stable material that forms a face-centered cubic (fcc) lattice at room temperature [12]. Within the fcc lattice positions, C_{60} molecules rotate rapidly in random, independent directions at 10^9–10^{10} Hz [13,14]. It has been shown that, at room temperature for monolayer films of C_{60} on Ag(111), the rapid rotation of C_{60} is repressed and the C_{60} ratchets slowly between preferred orientations. For monolayer films of C_{60} atop Cu(111), the C_{60} does not rotate at all. For bilayer films, however, the C_{60} molecules in the second layer rotate rapidly, just as they do in their fcc lattice [15,16]. Sliding friction measurements upon monolayers and bilayers of C_{60} therefore allows for direct experimental comparisons of the rapid and repressed rotational states.

The implications of our results transcend far beyond the particular experimental systems studied, as a fundamental knowledge of friction in adsorbed films [17] underlies a vast range of fundamental and applied issues in physics and nanotechnology. Examples include both the fundamental origins for the existence of static friction [18] and the design of atomic-scale automobiles [2].

We have performed quartz crystal microbalance (QCM) measurements of the friction levels for molecularly thin methanol films sliding along C_{60} monolayers and bilayers in these rapid and repressed rotational states (see Fig. 1) and report herein our observation that rapid rotation is associated with an increase in friction. A control experiment has also been performed: At temperatures close to $\sim$260 K, C_{60} undergoes a change of phase into a rotationally repressed phase in which it ratchets very slowly between preferred orientations [19,20]. Therefore, both C_{60} monolayers and bilayers are in a repressed rotational state

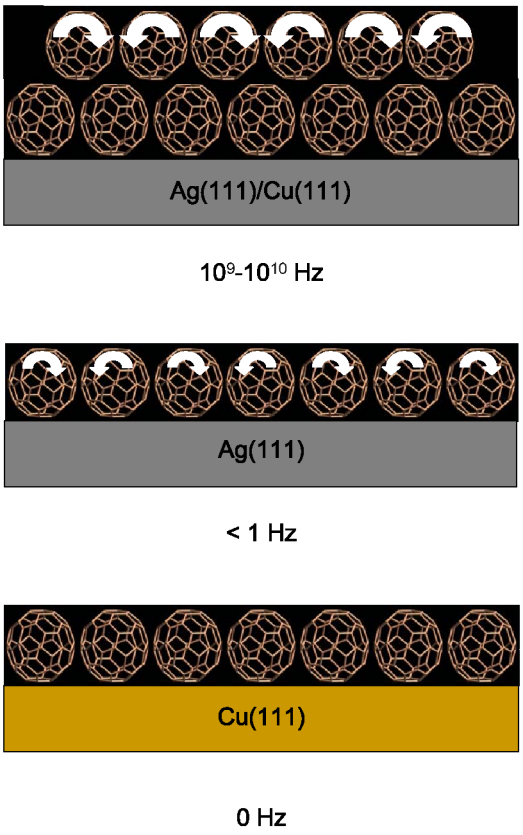

FIG. 1 (color online). Schematic of the QCM experiment. On Ag(111) or Cu(111), C_{60} molecules in the 2nd layer will rotate rapidly in random, independent directions, with rotational diffusion constants of 1.8×10^{10} s^{-1} [8,11]. On Ag(111), C_{60} molecules in the 1st layer will ratchet slowly between preferred orientations. On Cu(111), C_{60} molecules in the 1st layer will not rotate [9,12].

at 77.4 K. In order to differentiate C_{60} rotation from spurious experimental effects, we have performed control experiments of the sliding friction levels of krypton adsorbed on monolayers and bilayers of C_{60} films at 77.4 K. The friction levels for these control systems are identical within experimental error.

The quartz crystal microbalances used in this work were cut and then overtone polished from a single quartz crystal at a specified set of angles termed the AT cut that allows transverse shear motion with a quality factor Q near 10^5 and resonant frequency $f = 8$ MHz. QCM is an important experimental tool for studying a myriad of static and dynamic physical phenomena, including tribology at atomistic length and time scales that are unattainable by other experimental means [21]. It is also an attractive technique for comparative studies of macroscopic and microscopic phenomena, owing to the high sliding speeds (up to 2 m/s) and shear rates at which the data are recorded [22]. Given that the QCM has much faster sliding speeds than LFM (~1 m/s vs 1.5 μm/s) and also probes shorter time scales, it is potentially more sensitive to the rotational rates of the C_{60} molecules.

QCM friction measurements were performed by adsorbing methanol or krypton under equilibrium conditions onto the surface electrodes of the oscillator. Film adsorption onto the microbalance produces shifts in both the frequency and amplitude of vibration, which are simultaneously recorded as a function of pressure. Changes in the resonant frequency of the microbalance (δf) are proportional to the fraction of the mass of the condensed film that is able to track the oscillatory motion of the underlying substrate. Amplitude shifts are due to frictional shear forces exerted on the surface electrode by the adsorbed film. Characteristic slip times τ, which are inversely proportional to friction, are determined via $\delta(Q^{-1}) = 4\pi\tau(\delta f)$ [23]. The friction law that governs this system is of the "viscous friction" form $F = -(m/\tau)v = -m\eta v$. In this relation, F is friction force, m is the mass of the adsorbed film, and v is the average film sliding speed. The slip time τ, which is inversely proportional to the friction level, is a characteristic time for friction to decrease to $1/e$ of the original sliding speed v, assuming that it has been pushed at constant speed and then released, allowing frictional forces to bring it to a stop. Longer slip times τ thus correspond to lower friction levels. [Amplitude shifts are converted to quality factor shifts $\delta(Q^{-1})$ through calibration with a gas that does not condense at 77.4 K [24].]

For the Cu(111) sample, the copper was deposited atop a QCM with a 20 nm titanium precoat, to produce an extremely flat copper electrode [25]. The base pressure of the vacuum system ranged from 8×10^{-11} to 5×10^{-10} Torr. Thermal evaporation was then used to deposit 60 nm of 99.999% pure Cu or 80 nm of 99.999% pure Ag atop the titanium precoat or blank QCM, respectively, producing a mosaic structure with a (111) fiber texture [26]. C_{60} substrates were prepared by thermally evaporating 1 or 2 monolayers of C_{60} atop the Cu(111) or Ag(111) electrode on a blank QCM.

All samples were immediately transferred *in situ* to the adsorption cell where they were electrically connected to an external Pierce oscillator circuit. Adsorption isotherms of krypton and methanol were then acquired for each sample. First, the samples were chilled to 77.4 K by submersion in a liquid nitrogen bath in preparation for the krypton isotherm. After the samples had come to thermal equilibrium, they were exposed to research grade krypton gas while frequency and amplitude shifts were monitored with increasing pressure. After acquisition of the krypton isotherm, the sample was warmed to room temperature and the krypton gas evacuated from the chamber. Samples were then exposed to research grade methanol gas while monitoring frequency and amplitude shifts with increasing pressure.

The krypton and methanol frequency shift and quality factor shift data were acquired for eight independent samples, four with a monolayer of rigid or ratcheting C_{60}

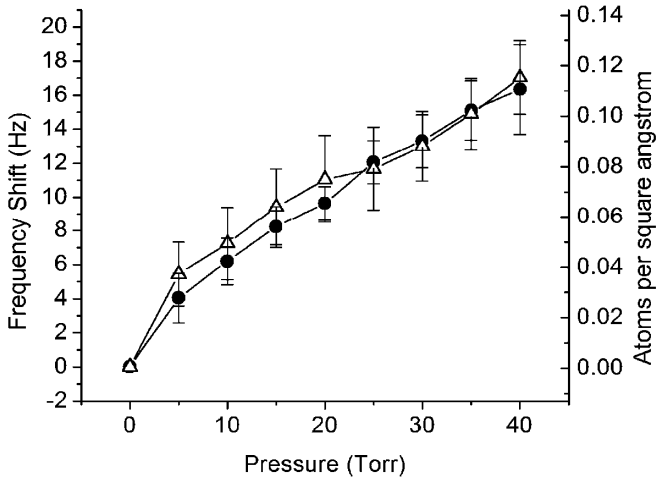

FIG. 2. Average methanol frequency shift and coverage data for four C_{60} monolayer (solid circles) and four C_{60} bilayer (open triangles) samples. The data sets for monolayer vs bilayer C_{60} were box-averaged to give a mean frequency shift, and the error bars represent 1 standard deviation from the mean.

and four with the bilayer of rotating C_{60}. The average methanol frequency shift and coverage data for the monolayer vs bilayer C_{60} samples is shown in Fig. 2. Examination of the frequency shift (mass uptake) data shows that the two curves lie atop one another, within the experimental error, indicating that the adhesion of methanol on rigid and slowly ratcheting vs rotating C_{60} systems is similar. If anything, the uptake of methanol on rotating C_{60} is slightly greater, indicating slightly higher adhesion for this system. There was no difference among the various monolayer C_{60} samples in methanol mass uptake data for rigid vs slowly ratcheting C_{60}.

The average slip times for methanol on monolayer (repressed rotation) vs bilayer (rapid rotation) C_{60} are shown in Fig. 3. Again, there was no difference between the 4 monolayer C_{60} samples, indicating that the methanol slippage was not dependent on whether the C_{60} was rigid or slowly ratcheting. Note that the methanol slipping on the monolayer C_{60} has longer slip times than the methanol slipping on the bilayer C_{60}. The slip times for a monolayer of methanol atop monolayer and bilayer C_{60} are 3.6 ± 1.2 and 1.9 ± 0.4 ns, respectively. The average slip times for krypton on monolayer vs bilayer C_{60} (both rigid) are shown in Fig. 4. The slip times for a monolayer of krypton atop monolayer vs bilayer C_{60} at 77.4 K are within experimental error, 3.1 ns $\pm$ 1.1 and 3.2 ns $\pm$ 0.6 ns, respectively.

Given the similarity of the 77.4 K data for krypton sliding on monolayer vs bilayer C_{60} films (neither of which are rotating), the differences in the room temperature methanol slip times on monolayer (not rotating) vs bilayer (rapidly rotating) C_{60} are not attributable to differences in surface morphology. The data instead link C_{60} rotation to increased friction (shorter slip times) in defiance of the ball-bearing analogy.

It is unlikely that the sliding of the methanol layer hinders in a significant manner the rotation of the C_{60} layer. A methanol molecule is more than 20 times less massive than a C_{60} molecule, and the sliding speed of the methanol is slow ($\sim$0.02 m/s) compared to the rapid rotation (10^9–10^{10} Hz) of the C_{60}. From an energetic point of

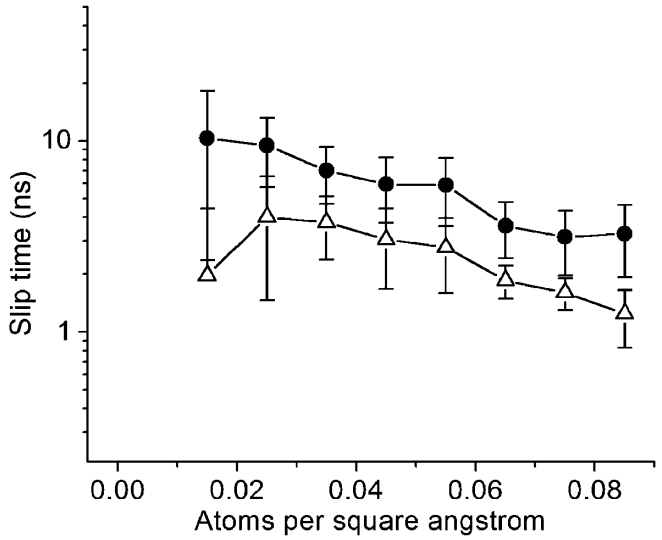

FIG. 3. The average slip times for methanol on monolayer C_{60} (solid circles) and bilayer C_{60} (open triangles) samples. The four data sets were box-averaged to give a mean slip time, and the error bars represent 1 standard deviation from the mean.

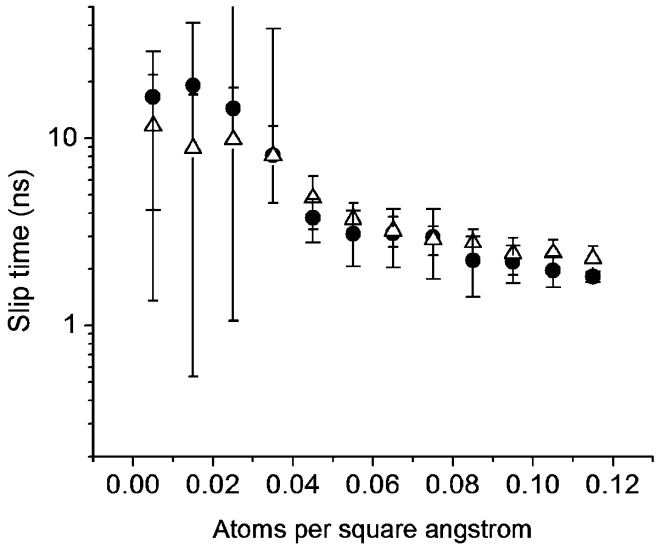

FIG. 4. The average slip times for krypton sliding on C_{60} monolayer (solid circles) and C_{60} bilayer (open triangles) films. The 4 data sets were box-averaged to give a mean slip time, and the error bars represent 1 standard deviation from the mean. Because of the box-averaging of the data, the liquid-solid transition usually present in krypton isotherms cannot be seen here, although it was present in the raw data sets.

view, the initial kinetic energy of the sliding methanol molecule is approximately 7 orders of magnitude smaller than the rotational kinetic energy of the C_{60} molecule, and the frictional energy dissipation per cycle is a fraction of that.

The observation of an increase in friction level requires detailed atomic-scale modeling in order to establish its origins, falling well beyond a direct mapping between macroscopic and microscopic physical properties. It is potentially explained within the context of phononic mechanisms for friction, whereby atomic lattice vibrations within the counterface materials are excited by the sliding action of the interface and are thus sensitive to the encounter rate of sliding counterface atoms.

Assuming the C_{60} molecules are fixed, as the methanol slides atop the C_{60}, it will encounter a certain number of carbon atoms in the C_{60} molecule per unit time. But if the C_{60} molecule is rotating as the methanol slides across the C_{60}, then this encounter rate increases. For experimentally realistic values (oscillation amplitude of 10–20 nm [22] and the frequency of oscillation of 8 MHz), we estimate that a methanol molecule slides over approximately 8 C_{60} molecules per cycle and the number of times that a methanol molecule would contact a carbon atom in the rotating C_{60} scenario would increase by a factor of approximately 10. A molecular dynamics simulation of the phononic friction in this system might well explain the experimental observations.

In summary, we have utilized QCM to measure friction levels for molecularly thin methanol films sliding along C_{60} substrates in rapid and repressed rotational states and have observed *increased* friction for the case of rapid rotation. The experiment, which is the first to link a change in friction to an identified rotation state of C_{60}, defies the ball-bearing analogy. We conclude that the phenomenon of nanomapping, while highly instructional and intuitive in nature, is speculative at best for predicting the behavior of nanoscale mechanical systems. While it is clear that nanoscale phenomena must underlie macroscale observables, rigorous atomic-scale modeling of the origins of the impact of molecular rotation on friction will be necessary to truly understand the observations reported here.

This work has been supported by the NSF, Grant No. DMR0320743, and AFOSR Grant No. F49620014-0132. K. Wahl and M. O. Robbins are thanked for many insightful discussions.

*Present address: Physics and Astronomy Department, Appalachian State University, 525 Rivers Street, Boone, NC 28608, USA.

[1] R. Feynman, Eng. Sci. **23**, 22 (1960).
[2] M. Porto, M. Urbakh, and J. Klafter, Phys. Rev. Lett. **84**, 6058 (2000).
[3] J. Cumings and A. Zettl, Science **289**, 602 (2000).
[4] J. W. Kang and H. J. Hwang, Nanotechnology **15**, 614 (2004).
[5] K. Miura, S. Kamiya, and N. Sasaki, Phys. Rev. Lett. **90**, 055509 (2003).
[6] M. H. Muser, Phys. Rev. Lett. **89**, 224301 (2002); P. Tangney, S. G. Louie, and M. L. Cohen, Phys. Rev. Lett. **93**, 065503 (2004).
[7] S. B. Legoas, R. Giro, and D. S. Galvao, Chem. Phys. Lett. **386**, 425 (2004).
[8] Q. Liang, O. K. C. Tsui, Y. Xu, H. Li, and X. Xiao, Phys. Rev. Lett. **90**, 146102 (2003).
[9] T. Coffey, M. Abdelmaksoud, and J. Krim, J. Phys. Condens. Matter **13**, 4991 (2001).
[10] L. Rapoport, Yu Bilik, Y. Feldman, M. Homyonfer, S. R. Cohen, and R. Tenne, Nature (London) **387**, 791 (1997).
[11] R. Greenberg, G. Halperin, I. Etsion, and R. Tenne, Tribol. Lett. **17**, 179 (2004).
[12] M. S. Dresselhaus, G. Dresselhaus, and P. C. Eklund, *Science of Fullerenes and Carbon Nanotubes* (Academic, San Diego, 1996).
[13] D. A. Neumann *et al.*, Phys. Rev. Lett. **67**, 3808 (1991).
[14] R. D. Johnson, C. S. Yannoni, H. C. Dorn, J. R. Salem, and D. S. Bethune, Science **255**, 1235 (1992).
[15] E. I. Altman and R. J. Colton, Surf. Sci. **295**, 13 (1993).
[16] T. Sakurai *et al.*, Appl. Surf. Sci. **87–88**, 405 (1995).
[17] T. Coffey and J. Krim, Phys. Rev. Lett. **95**, 076101 (2005).
[18] G. He, M. H. Muser, and M. O. Robbins, Science **284**, 1650 (1999).
[19] P. A. Heiney, J. E. Fischer, A. R. McGhie, W. J. Romavow, A. M. Denenstein, J. P. McCauley, Jr., A. B. Smith, III, and D. E. Cox, Phys. Rev. Lett. **66**, 2911 (1991).
[20] R. Tycko, R. C. Haddon, G. Dabbagh, S. H. Glarum, D. C. Douglass, and A. M. Mujsce, J. Phys. Chem. **95**, 518 (1991).
[21] J. Krim, Am. J. Phys. **70**, 890 (2002).
[22] B. Borovsky, B. L. Mason, and J. Krim, J. Appl. Phys. **88**, 4017 (2000).
[23] J. Krim and A. Widom, Phys. Rev. B **38**, 12 184 (1988).
[24] E. T. Watts, J. Krim, and A. Widom, Phys. Rev. B **41**, 3466 (1990).
[25] S. M. Lee and J. Krim (to be published).
[26] K. K. Kakati and H. Wilman, J. Phys. D: Appl. Phys. **6**, 1307 (1973).